An Experimental Study of the Flow Around an Axisymmetric Body at High Angles of Attack

D.K. Pantelatos*, D.S. Mathioulakis**
*Hellenic Air Force General Staff
C2 Directorate, Papagos Camp 15500, Athens, Greece
**National Technical University of Athens
Department of Mechanical Engineering, Fluids Section
Heroon Polytechniou 9, Zografos 15773, Athens, Greece

Introduction

The investigation of the flow field around an axisymmetric body inclined at an angle with respect to the oncoming free stream constitutes a challenging task due to the complex nature of the flow. However, understanding the unanswered yet question concerning the basic reason that causes flow asymmetries over an apparently symmetric body at high angles of attack would improve maneuverability of bodies of such shapes. A good number of applications concerning flight of both commercial and military airplanes at high angles of attack and the associated problems of flow control are included in Ref.1. Pressure measurements over an ogive cylinder for a wide range of angles of attack α and Re are presented in Ref.2, showing the change of the flow character from laminar to transitional and to turbulent as a function of α and Re. In Ref.3 the asymmetric vortices over an inclined ogive cylinder were visualized by using smoke in a wind tunnel at $Re=3x10^4$ and the side force was measured by strain gauge balances. In Ref.4 the lee side of a cylinder was visualized in a water tunnel including details of the flow topology. Comprehensive reviews of this subject can be also found in Ref.5 and 6.
In the present work the flow field about a blunted nose cylinder was studied at various pitch and yaw angles by carrying out pressure measurements, employing an oil film and smoke flow visualization techniques.

Experimental Set-up

The flow field about an axisymmetric body was examined at various angles of attack in the closed circuit subsonic wind tunnel of the Aerodynamics Laboratory of NTUA. The model was machined out of aluminum, having a blunted nose (spherical surface) and circular cross sections thereafter, the diameter of which increased progressively to the model's base diameter D =127mm (Fig.1a).

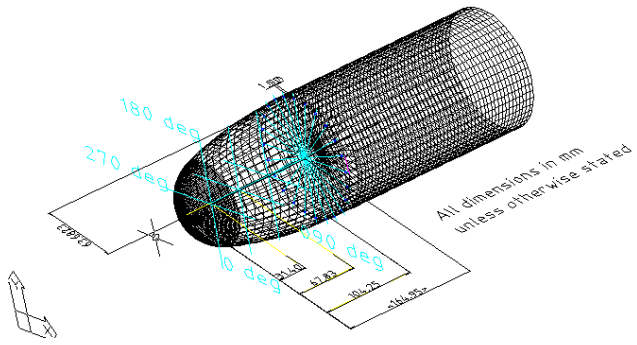

Figure 1a

Paper presented at the RTO AVT Symposium on "Advanced Flow Management: Part A – Vortex Flows and High Angle of Attack for Military Vehicles", held in Loen, Norway, 7-11 May 2001, and published in RTO-MP-069(I).

Report Documentation Page

Form Approved
OMB No. 0704-0188

1. REPORT DATE	2. REPORT TYPE	3. DATES COVERED
00 MAR 2003	**N/A**	**-**

4. TITLE AND SUBTITLE	5a. CONTRACT NUMBER
An Experimental Study of the flow Around an Axisymmetric Body at High Angles of Attack	5b. GRANT NUMBER
	5c. PROGRAM ELEMENT NUMBER
6. AUTHOR(S)	5d. PROJECT NUMBER
	5e. TASK NUMBER
	5f. WORK UNIT NUMBER
7. PERFORMING ORGANIZATION NAME(S) AND ADDRESS(ES) **NATO Research and Technology OrganisationBP 25, 7 Rue Ancelle, F-92201 Neuilly-Sue-Seine Cedex, France**	8. PERFORMING ORGANIZATION REPORT NUMBER
9. SPONSORING/MONITORING AGENCY NAME(S) AND ADDRESS(ES)	10. SPONSOR/MONITOR'S ACRONYM(S)
	11. SPONSOR/MONITOR'S REPORT NUMBER(S)

12. DISTRIBUTION/AVAILABILITY STATEMENT
Approved for public release, distribution unlimited

13. SUPPLEMENTARY NOTES
Also see: ADM001490, Presented at RTO Applied Vehicle Technology Panel (AVT) Symposium held inLeon, Norway on 7-11 May 2001, The original document contains color images.

14. ABSTRACT

15. SUBJECT TERMS

16. SECURITY CLASSIFICATION OF:			17. LIMITATION OF ABSTRACT	18. NUMBER OF PAGES	19a. NAME OF RESPONSIBLE PERSON
a. REPORT	b. ABSTRACT	c. THIS PAGE			
unclassified	**unclassified**	**unclassified**	**UU**	**12**	

Standard Form 298 (Rev. 8-98)
Prescribed by ANSI Std Z39-18

The total length of the model was 500mm and its projected area to the tunnel's cross section ($1.8x1.4m^2$) was less than 5%. In order to record both the longitudinal and circumferential surface pressure distributions, pressure holes were opened along a generator as well as circumferentially along four sections in the nose area, named sections A,B,C,D, respectively. An electric motor installed at the very end of the model rotated it about its longitudinal axis, thus allowing pressure measurements over the whole surface of the body (Fig.1b). This rotation of the model reduced significantly the number of the pressure taps, minimizing their influence upon the flow development over the model surface. A 48 port scanivalve was installed inside the model in order for the length of the tubing which connected the pressure taps to the pressure transducer be short and avoid long transients when moving from one pressure hole to another. The analog output of the scanivalve was the difference of the local static pressure from the static pressure of the oncoming free stream, the latter being measured by a Pitot-Static tube, located upstream of the model. The angle of attack of the model was adjusted either by changing its pitch angle or its yaw angle or a combination of these two. The pitch angle (the angle of the model axis with respect to the horizontal axis of the tunnel test section) was adjusted by an electric motor (Fig.1b) whereas the yaw angle by the rotating sting of the six- component balance of the tunnel upon which the model was mounted.

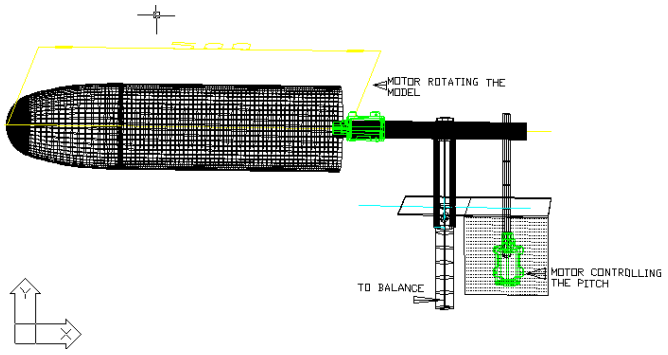

Figure 1b

Experimental Procedure

The experiments were carried out for $Re=1.85x10^5$ and for angles of attack α, 0^0 to 40^0. Although Re was small compared to cases met in practice, it was decided to keep it low since as it has been shown before (Ref.2), flow asymmetries for ogive cylinders are very significant for this Re as well as for one order of magnitudes higher Re ($2x10^6$). In between, these asymmetries are dampened out due to the transitional behavior of the flow. Therefore, increasing Re to about $0.6x10^6$ which was the maximum possible value for this tunnel it would not help seeing any flow asymmetries. However, it is worth mentioning that not only side force coefficients versus angle of attack are similar despite this big difference in Re but their distribution along the body is also similar (Ref.2). As mentioned in (Ref.5) experiments at Re below $3x10^5$ require that free stream turbulence level be low (at most 0.1%) in order to avoid any suppression of flow asymmetries. In our case this was 0.2%. It is also added that free stream is not responsible for flow asymmetries, although this might destroy the stable character of these asymmetries.

Static pressures were measured at 47 points on the surface of the body along a generator as well as along the periphery of sections A, B, C, D. Pressure measurements were repeated by rotating the model about its axis with steps of 30^0, until a complete turn was complete. Mean values of pressure coefficients c_p based on the free stream dynamic pressure are shown in the subsequent figures as a function of the distance x (in mm) from the nose and/or the azimuthal angle φ. The generator $\varphi=0$ corresponds to the windward side symmetry plane and increases in the anticlockwise direction, looking at the model from an upstream location (Fig.1).

Besides pressure measurements, oil film flow visualization was also employed in order to record the shape of both the limiting and separation lines. By putting small droplets of a mixture of oil and titanium dioxide on the surface of the model the formed streaky pattern was then pictured after the end of the experiment. In addition to that a smoke probe and laser light sheet were used to illustrate the nature of the vortical behavior at an angle of attack of 40 degrees, at a location of azimuthal angle φ = 120 deg and x= 280 mm.

Results and Discussion

Pressure measurements for zero yaw angle

For zero yaw angle and pitch angles 20^0 and 40^0, which correspond to α= 20^0 and 40^0 respectively, the pressure distributions presented similarities and differences. Fig.2 and 3 show pressure distributions at sections A, B, C, D in the nose area versus φ.

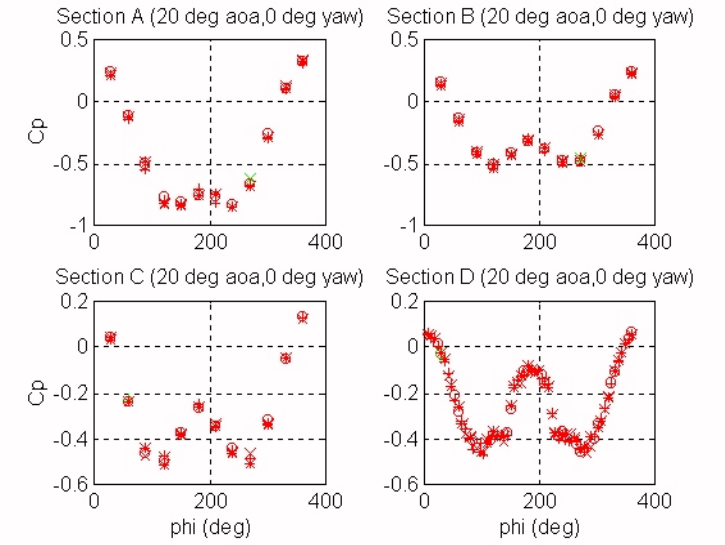

Figure 2

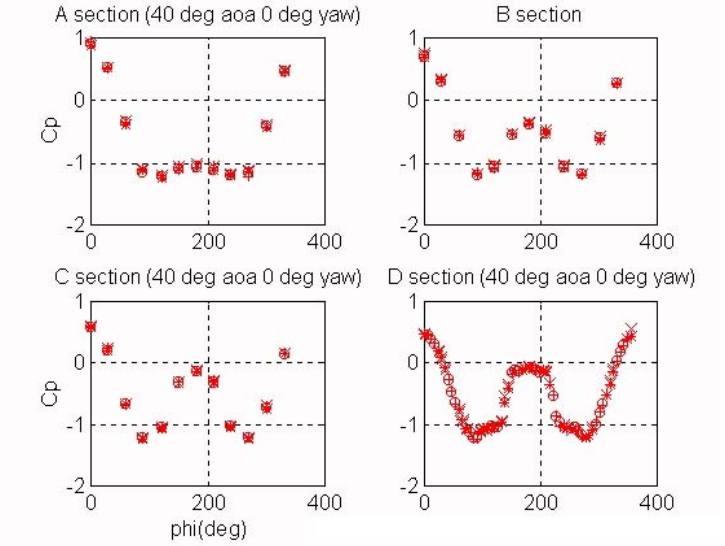

Figure 3

In these diagrams different symbols correspond to pressures obtained from different pressure taps. Especially at sections A, B and C there were four pressure taps 90^0 apart, in order to be able to detect any asymmetries, if they existed, by simultaneously measuring pressures at symmetric points, without rotating the model. At section D, it was decided to open more pressure holes since this section was at the end of the curved nose area and therefore the influence of these holes to the flow development thought to be minimal. Since there were more than one hole in each of these four sections the pressure at a given azimuthal position was obtained more than one times. It was thus possible to check the repeatability of the results or their deviation that did not exceed for c_p the value of 0.1 from the local mean value.

A basic difference between $\alpha=20^0$ and $\alpha=40^0$ is that for the lower α, the pressures are smaller. However, the shape of the distributions was similar. Namely, starting from $\varphi=0^0$ (at the windward symmetry plane), where c_p takes its maximum value, this drops to a minimum at a certain φ location dependent upon the cross section and the angle of attack. Very close to the nose this pressure suction peak is located at $\varphi=180^0$ (lee side symmetry plane), moving progressively to smaller φ's at downstream cross sections. For example Fig.2 and 3 show that for sections A through D this angle changes from 150^0 to 100^0 for $\alpha=20^0$, whereas for $\alpha=40^0$ the corresponding locations are 120^0 to 90^0. Further downstream, where there is no surface curvature along the model's axis, pressure suction peak appears earlier, namely for $\alpha=20^0$ at $\varphi=80^0$ and for $\alpha=40^0$ at $\varphi=60^0$. Excluding a very small region close to the nose, the pressure after taking its minimum value it increases again, taking a local maximum at $\varphi=180^0$. This is shown in detail in section D, where the number of measurements is maximum compared to all other cross sections. Namely, next to pressure minimum there is a small pressure recovery, accompanied by a plateau, then a second significant this time recovery and a second plateau at the lee side symmetry plane. This pressure distribution suggests that the cross flow boundary layer separates and reattaches (first plateau). After reattachment, the flow becomes turbulent causing a positive pressure gradient leading to separation again at $\varphi=150^0$. A similar behavior has been also observed over ogive cylinders at an angle of attack (Ref.6). For the above two cases, the longitudinal pressure distributions along four generators namely, $\varphi=0$, 90^0, 180^0 and 270^0 are shown in Fig.4a and b.

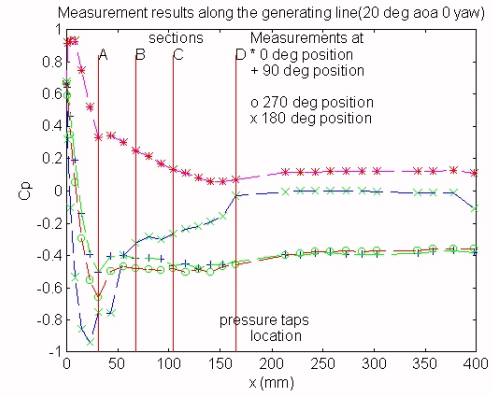

Figure 4a

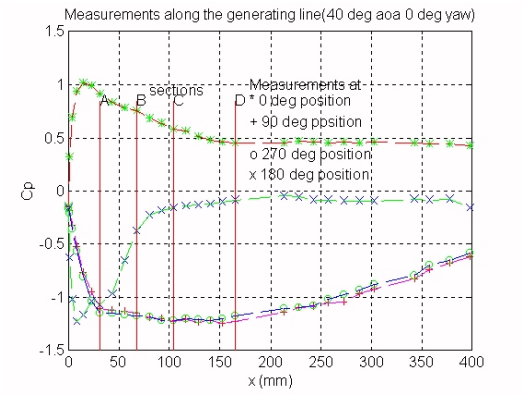

Figure 4b

As expected significant pressure gradients appear in the curved (streamwise) portion of the body and particularly in the spherical area. Some basic remarks based on Fig.4 are as follows:
a) Whether flow asymmetry exists or not this can be concluded through the pressure distributions along $\varphi=90^0$ and $\varphi=270^0$, namely on the right and left with respect to the symmetry plane. We notice that for $\alpha=20^0$ there is some asymmetry in the nose area but further downstream this disappears. According to (Ref.2) the side force distribution increases with x, which here it does not. On the contrary, for $\alpha=40^0$ it seems that the flow is essentially symmetric for $\varphi=90^0$ and $\varphi=270^0$ within of course the experimental accuracy. Therefore, for the examined cases there is no strong evidence that any flow asymmetries are systematic. This was also verified for the majority of the examined combinations of pitch and yaw angles.
b) Along the generator $\varphi=180^0$, there is a plateau close to section A for both angles of attack, downstream of which there is a pressure recovery, suggesting the appearance of a bubble in this area. The difference between $\alpha=20^0$ and $\alpha=40^0$ is that this bubble is located a little upstream for the higher angle of attack.
c) Due to flow symmetry the stagnation point is located in the windward side along the generator $\varphi=0^0$, where c_p takes its maximum value of 1. An increase of α from 20^0 to 40^0 moves this point from x=4mm to a downstream station x=15mm.
d) The increase of the angle of attack increases the pressure difference between the windward and leeward side and consequently the normal force.

Pressure measurements for non zero yaw angle

According to Ref. 11 rapid maneuvers at high angles of attack for the high performance aircraft and missiles, causes the vehicles to be subject to unsteady separated highly nonlinear aerodynamics with strong coupling between longitudinal and lateral degrees of freedom. This cross coupling exists even at zero angle of sideslip for high angles of attack where the flow separation becomes asymmetric on a slender forebody. This can result in dynamic instability of aircraft and missiles through dynamic cross coupling effects .

The strong coupling between vehicle motion and flow separation causes this situation called moving wall effect.

Disregarding the moving wall effect the apparent three-dimensional motion of the vehicle could be " decoupled" by gradually increasing yaw angle for a given pitch angle. According to that, experiments were carried out for various pitch angles (0^o to 30^o deg) and yaw angles (0^o to 30^o deg). The basic conclusion drawn from the cases examined is that for a given pitch angle during the escalation of the yaw angle the azimuthal pressure diagrams are displaced along the axis of φ. This is due to the fact that by increasing the yaw angle the symmetry plane does not go any more through $\varphi=0$ and $\varphi=180^0$ but it is tilted a certain angle, which is related to the pitch and

yaw angles. Of course at the same time the angle of attack changes as well. The relationships of these angles are easily found based on simple geometric relations, namely:
$\cos(\alpha)=\cos(p)*\cos(y)$,
where α, is the angle of attack, p, is the pitch angle and y, is the yaw angle. Also the angle φ_1 by which the symmetry plane is tilted with respect to the axis $\varphi=90^0$, 270^0 is given by:
$\sin\varphi_1=\sin p*\cos y/\sin\alpha$.
The above are clearly shown in Fig.5 in which for $p=20^0$ the pressure distributions in section D are displaced along the axis φ for yaw angles of 0, 10^0 and 30^0 (red, blue, green) without again presenting any asymmetries with respect to the symmetry plane of each case which goes through the two pressure maximum.

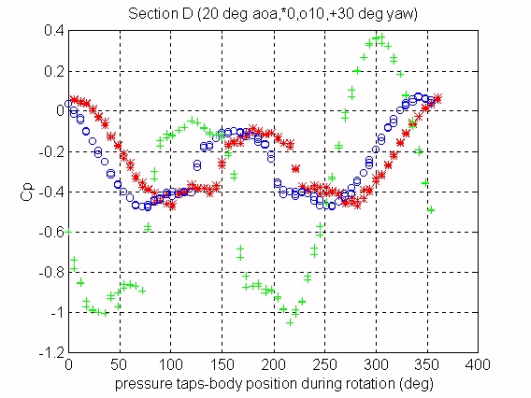

Figure 5

Additionally according to Ref. 11 for a pointed ogive cylinder with similar L/D ratio (were L is the length from the nose and D is the diameter) with the one under examination, the asymmetric vortex shedding should start at α = 32.5 deg and for a blunted cone - cylinder body the asymmetric flow separation and associated vortex shedding occurs first on the aftbody at α = 23 and 7.5 deg for L/D = 10.3 and 32 respectively. We can comment on that, noting that the greater the L/D ratio and the "sharpest" the nose of the model, the lower the angle of attack in which the asymmetric vortex shedding appears.

In our case (blunted nose model) and according to the results mentioned above, the range of the pitch and yaw angles in which the subject model was examined, restricts the asymmetric flow from occurring.

However, for 40^o pitch and 0^o yaw angles, the model was subject to asymmetric flow observed mainly in its aftbody, starting from length 350 mm and beyond (figures 6 and 7). This does not contradict figure's 4b comments because the subject flow asymmetry is located in the leeside part of the model between 100^o and 250^o azimuthal angles φ.

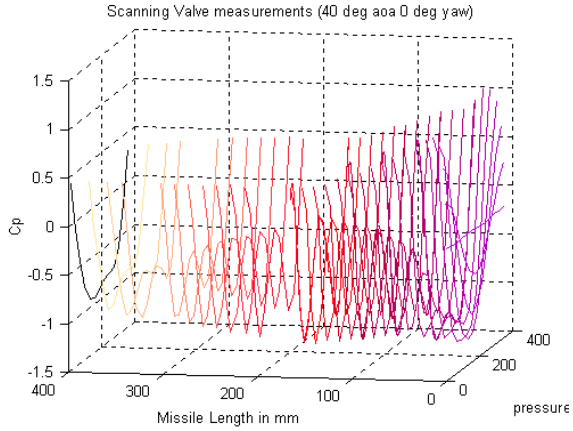

Figure 6

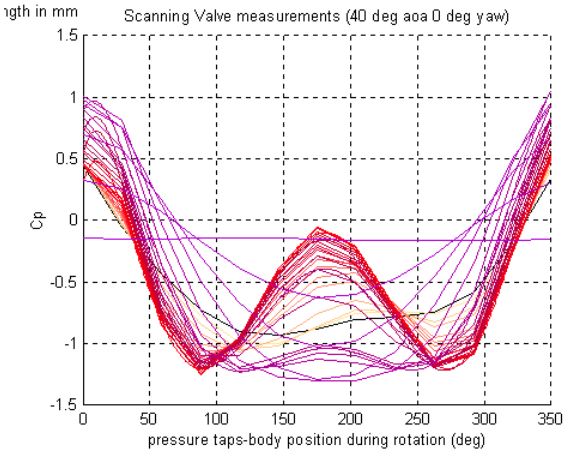

Figure 7

Flow visualization results

Details of the flow next to the body surface were also revealed by recording the shapes of the streak lines produced by a mixture of oil and TiO_2 (used in our study) which coincide in practice with the limiting streamlines (Ref.10). In the case of the so called open separation these lines merge on both sides of the separation line (Ref.7,8,9). One of the two separating lines for $\alpha=40^0$ is shown in Fig.8. Namely, limiting streamlines start from both the windward and leeward symmetry plane and they meet along a line that does not follow a generator. More specifically, this separation line in the nose area goes through locations $\varphi>90^0$ while close to the end of the model this goes through $\varphi<90^0$. It should be reminded that the pressure holes seen in the nose area are located along the generator $\varphi=90^0$. This picture agrees with the corresponding pressure distribution according to which the pressure suction peak and the next to it plateau follows the same course. In Fig.9, a detailed picture is shown for the same angle of attack in the leeside in the nose area. The limiting streamlines start from the stagnation point and they move up to a line normal to the axis of the model where they stop like meeting a barrier. This is apparently the location where a bubble exists which in the longitudinal pressure distribution is presented as a local plateau. Exactly downstream of this barrier there is a semicircle line which most probably coincides with the trace of the horn vortex (Ref.9). Reducing the angle of attack to $\alpha=30^0$, this bubble is met at a downstream station (Fig.10). Finally, for $\alpha=10^0$ contrary to what was expected, these lines seem to be met at the windward side (Fig.11 and 12). Repeating the flow visualization

for even smaller angles it proved to be gravity, which influence the shape of the lines, giving that erroneous results. Therefore the results of this technique need careful interpretation.

Figures 8&9

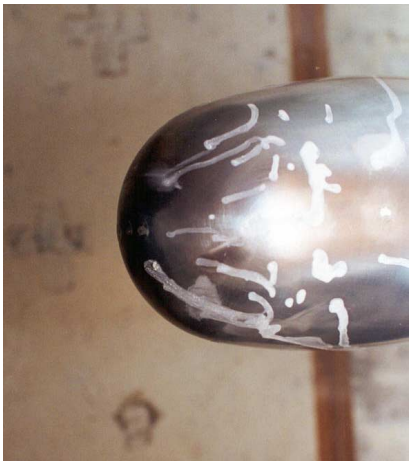

Figure 10

Figures 11&12

In order to visualize the separation and reattachment of the flow discussed in figures 4a and b, for an angle of attack of 40 degrees, a smoke probe was attached on the model, and a laser light sheet vertical to the model's longitudinal axis, enhanced the smoke presence. The visualization results were videotaped. In Fig.13 an example of this visualization is presented showing the clockwise helical spinning of the flow at a location around an azimuthal angle φ= 120 deg and x= 280 mm, that probably leads to its reattachment towards the model's leeside surface.

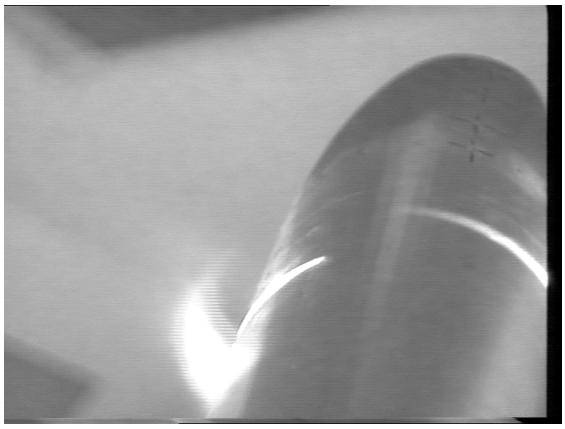

Figure 13

Conclusions

Based on pressure measurements and flow visualization the flow field around a blunted nose cylinder at angles of attack up to 40^0 and Re=1.85×10^5 had the following characteristics:

a) Any flow asymmetries were not systematic, a fact that agrees with the general experience that cylinders with pointed noses are most susceptible to flow asymmetries.
b) Along the circumferential direction there are two pressure plateau, one close to 90^0 far from the stagnation point generator (depending on the angle of attack and the distance from the nose) and the other one at the lee symmetry plane, suggesting the existence of

two separation regions. The separation lines do not follow a generator, being closer to the leeside symmetry plane in the nose area and moving far from it in the afterbody.

c) In the longitudinal direction along the leeside symmetry plane, starting from the nose, the pressure is favorable (in the spherical nose surface), then there is a small plateau and next it becomes positive until eventually in the afterbody it becomes level.

d) Keeping the pitch angle constant and increasing the yaw angle, the flow remains symmetric with the only difference that the axis of symmetry is tilted a certain angle, being a function of the yaw and pitch angles.

Acknowledgements

The authors wish to express their gratitude to the Hellenic Air Force and to the Hellenic Aerospace Industry for their support.

References

1. Erickson G.E. 1995. High angle-of-attack aerodynamics. Annu. Rev. Fluid Mech. 27.pp.45-88.
2. Lamont P.J. 1982. Pressures around an inclined ogive cylinder with laminar, transitional, or turbulent separation. AIAA J.20.No.11.pp.1492-1499.
3. Zilliac G.G, Degani D., Tobak M. 1991. Asymmetric vortices on a slender body of revolution. AIAA J. 29.No 5.pp.667-675.
4. Ward K.C. and Katz J. 1989. Development of flow structures in the Lee of an inclined body of revolution. J. Aircraft. 26.No.3.pp.198-206.
5. Champigny P.1994. High angle of attack aerodynamics. Presented at an AGARD Special Course on “Missile aerodynamics”.pp.5.1-5.19.
6. Agardograph 323. 1994. Scale effects on aircraft and weapon aerodynamics.
7. Wang K.C. 1972. Separation patterns of boundary layer over an inclined body of revolution. AIAA J.10.No8.pp.1044-1050.
8. Costis C.E., Hoang N.T. and Telionis D.P. 1989. Laminar separating flow over a prolate spheroid. J Aircraft.26.No.9.pp.810-816.
9. Tobak M., Peake D.J. 1982. Topology of three dimensional separated flows. Ann. Rev. Fluid Mech.14.pp.61-85.
10. Techniques of flow visualization. Agardograph 302.
11. Erickson L.E. 1993. Unsteady Flow Separation on Slender Bodies at High Angles of Attack. Journal of Spacecraft and Rockets vol 30 No 6 Sep.- Nov. 93

Paper: #4
Author: Lt. Col. Pantelatos

Question by Dr. Luckring: This is just a comment. There is a paper published by Susan Ying in the Williamsburg Applied Aero Conference (ca. 1988). She showed Navier Stokes calculations for a similar geometry that may be useful for interpreting your flow patterns.

Answer: Thank you.

This page has been deliberately left blank

———————

Page intentionnellement blanche